Supplementary Information

A highly luminescent copper (I) halide complex scintillator for X-ray imaging application

Xun-Yang Chen, [a] Jun-Hua Wei,*[a] Zi-Lin He, [a] Jing-Hua Chen, [a] Xuejing Wang,[b] Liang Li,[b] Dai-Bin Kuang*[a]

[a] Key Laboratory of Bioinorganic and Synthetic Chemistry of Ministry of Education, Lehn Institute of Functional Materials, GBRCE for Functional Molecular Engineering, School of Chemistry, IGCME, Sun Yat-sen University, Guangzhou, China.

[b] Macao Institute of Materials Science and Engineering (MIMSE), Macau University of Science and Technology, Taipa, Macao 999078, China

*Corresponding author: Jun-Hua Wei (weijh39@mail.sysu.edu.cn), Dai-Bin Kuang (kuangdb@mail.sysu.edu.cn).

Table S1. Single crystal structural refinement results for $Cu_2I_2L_2$.

Compound	**$Cu_2I_2L_2$**
Empirical formula	$C_{26}H_{36}CuINP$
Formula weight	583.97
Temperature/K	100.04
Crystal system	monoclinic
Space group	C2/c
a/Å	19.6838(11)
b/Å	13.0306(11)
c/Å	20.3708(12)
α/°	90
β/°	105.397(3)
γ/°	90
Volume/Å3	5037.4(6)
Z	8
ρ_{calc}/g cm^{-3}	1.540
μ/mm^{-1}	2.170
F(000)	2368.0
Radiation	MoKα (λ = 0.71073)
2Θ range for data collection/°	5.116 to 55.1
Index ranges	$-25 \leq h \leq 25$, $-16 \leq k \leq 16$, $-26 \leq l \leq 26$
Reflections collected	36656
Independent reflections	5817 [R_{int} = 0.0706, R_{sigma} = 0.0407]
Data/restraints/parameters	5817/0/273
Goodness-of-fit on F^2	1.052
Final R indexes [I >= 2σ (I)]	R_1 = 0.0321, wR_2 = 0.0683
Final R indexes [all data]	R_1 = 0.0411, wR_2 = 0.0746
Largest diff. peak/hole / e Å^{-3}	0.71/-0.67

Table S2. Single crystal structural refinement results for $Cu_2Br_2L_2$.

Compound	**$Cu_2Br_2L_2$**
Empirical formula	$C_{26}H_{36}BrCuNP$
Formula weight	536.97
Temperature/K	142.86
Crystal system	monoclinic
Space group	$P2_1/c$
a/Å	11.2439(4)
b/Å	21.8051(9)
c/Å	9.9203(4)
α/°	90
β/°	93.8560(10)
γ/°	90
Volume/Å^3	2426.70(16)
Z	4
ρ_{calc}/g cm^{-3}	1.470
μ/mm^{-1}	2.626
F(000)	1112
Radiation	MoKα (λ = 0.71073)
2Θ range for data collection/°	4.52 to 55.30
Index ranges	$-14 \leq h \leq 13$, $-28 \leq k \leq 28$, $-12 \leq l \leq 12$
Reflections collected	33093
Independent reflections	5636 [R_{int} = 0.0529, R_{sigma} = 0.0372]
Data/restraints/parameters	5636/159/328
Goodness-of-fit on F^2	1.033
Final R indexes [I >= 2σ (I)]	R_1 = 0.0259, wR_2 = 0.0643
Final R indexes [all data]	R_1 = 0.0301, wR_2 = 0.0665
Largest diff. peak/hole / e Å^{-3}	0.56/-0.42

Table S3. Single crystal structural refinement results for $Cu_2Cl_2L_2$.

Compound	**$Cu_2Cl_2L_2$**
Empirical formula	$C_{26}H_{36}ClCuNP$
Formula weight	492.52
Temperature/K	100.0
Crystal system	monoclinic
Space group	$P2_1/c$
a/Å	11.2079(9)
b/Å	21.6510(17)
c/Å	9.9046(9)
α/°	90
β/°	94.633(3)
γ/°	90
Volume/Å^3	2395.6(3)
Z	4
ρ_{calc}/g cm^{-3}	1.366
μ/mm^{-1}	1.104
F(000)	1040.0
Radiation	MoKα (λ = 0.71073)
2Θ range for data collection/°	4.534 to 52.934
Index ranges	$-14 \leq h \leq 14$, $-27 \leq k \leq 27$, $-12 \leq l \leq 12$
Reflections collected	51201
Independent reflections	4946 [R_{int} = 0.0633, R_{sigma} = 0.0302]
Data/restraints/parameters	4946/253/327
Goodness-of-fit on F^2	1.033
Final R indexes [I>=2σ (I)]	R_1 = 0.0303, wR_2 = 0.0701
Final R indexes [all data]	R_1 = 0.0380, wR_2 = 0.0747
Largest diff. peak/hole / e Å^{-3}	0.73/-0.42

Table S4. Contribution of molecular orbital transitions of $S_0 \rightarrow S_1$ and $S_0 \rightarrow T_1$ transitions.

	molecular orbital transitions	proportion
$S_0 \rightarrow S_1$ transition	HOMO-3 → LUMO+1	24.8%
	HOMO → LUMO+2	24.1%
	HOMO-1 → LUMO+4	23.0%
	HOMO-2 → LUMO+7	16.1%
$S_0 \rightarrow T_1$ transition	HOMO-4 → LUMO+2	8.5%
	HOMO-5 → LUMO+4	8.0%
	HOMO-6 → LUMO+1	6.6%
	HOMO-9 → LUMO	6.2%
	HOMO-11 → LUMO+5	5.5%

Table S5. Summary of the properties related to X-ray detection and imaging of organic-inorganic hybrid scintillators.

Material	Light Yield (photons/MeV)	LOD (nGy/s)	Resolution	Reference
$(C_{18}H_{34}P_2)MnBr_4$	79800	72.8	0.322 mm	1
$(C_{21}H_{22}P)_2MnBr_4$	46786	217.7	20 lp/mm	2
$(TBA)_2MnCl_4$	21000	381	5.6 lp/mm	3
$(Bmpip)_2Cu_2Br_4$	16000	710	-	4
$(DIET)_3Cu_3Br_3$	20000	189	11.7 lp/mm	5
$(DBA)_4Cu_4I_4$	12842	-	5 lp/mm	6
$(ETPP)_2Cu_2I_4$	23200	150.9	16 lp/mm	7
$Cu_2I_2L(PPh_3)_2$	12950	42.5	17.3 lp/mm	8
Cu_4I_4(3-methylpyridine)$_4$	55069	240	-	9
$Cu_2I_2L_2$	38297	49.4	10 lp/mm	This work

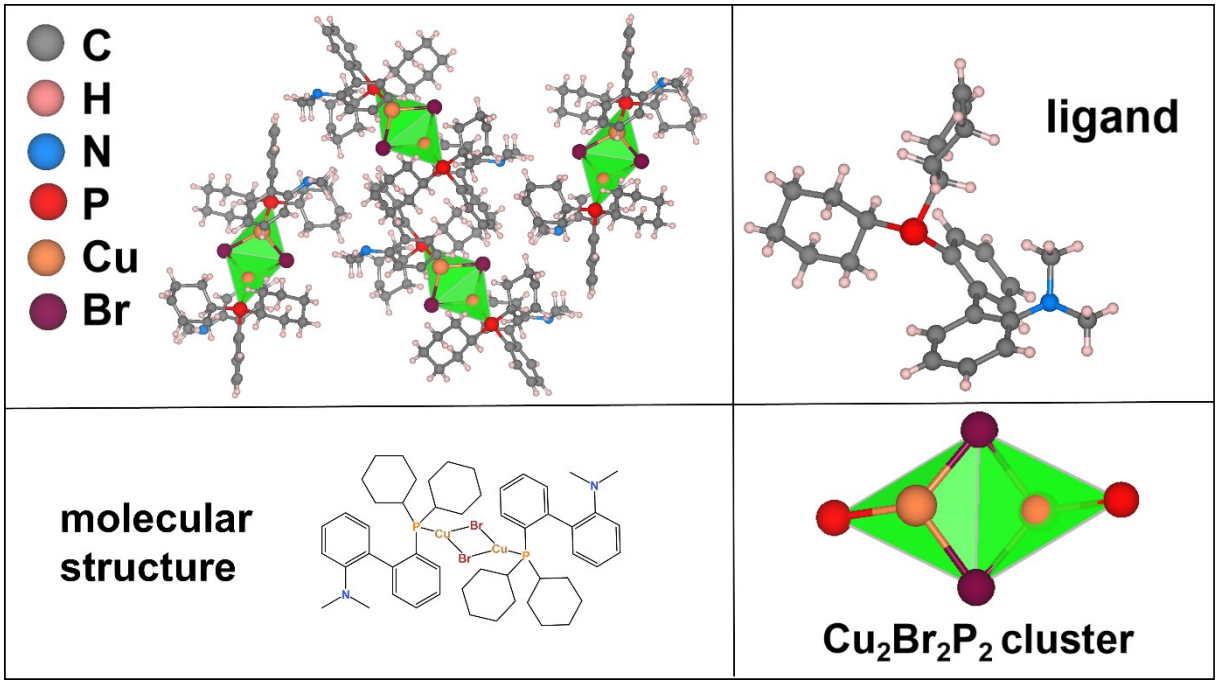

Figure S1. Single crystal structure of $Cu_2Br_2L_2$ (Disordered atoms have been deleted for clarity).

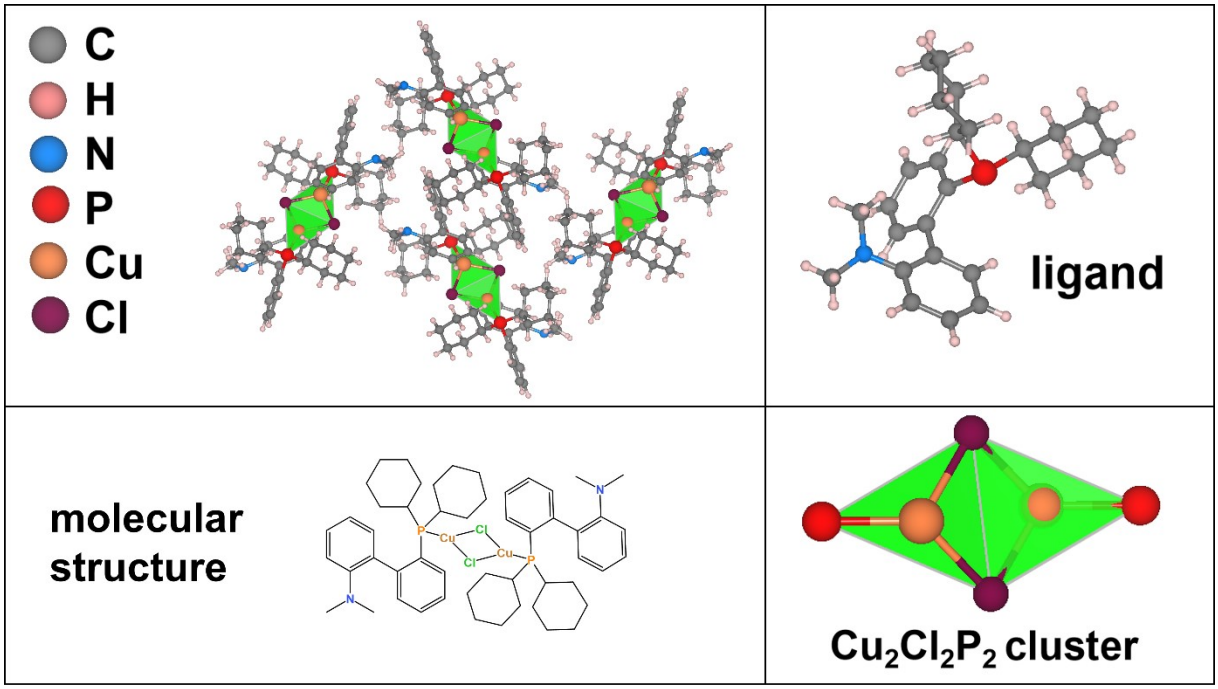

Figure S2. Single crystal structure of $Cu_2Cl_2L_2$ (Disordered atoms have been deleted for clarity).

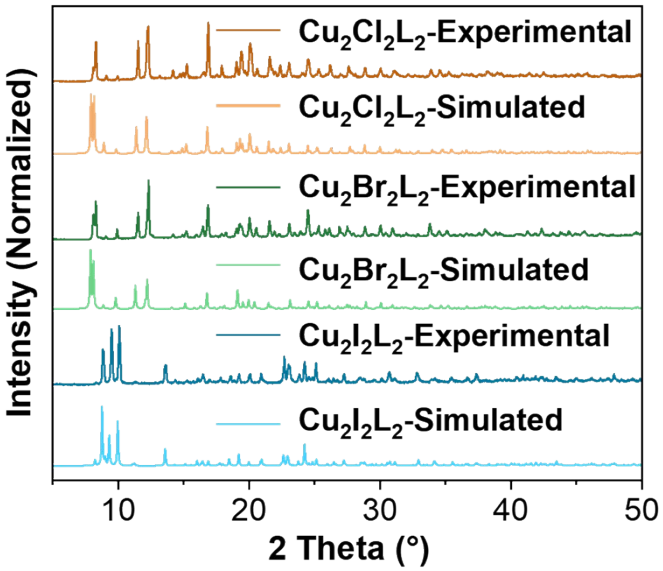

Figure S3. Simulated and PXRD patterns of $Cu_2X_2L_2$.

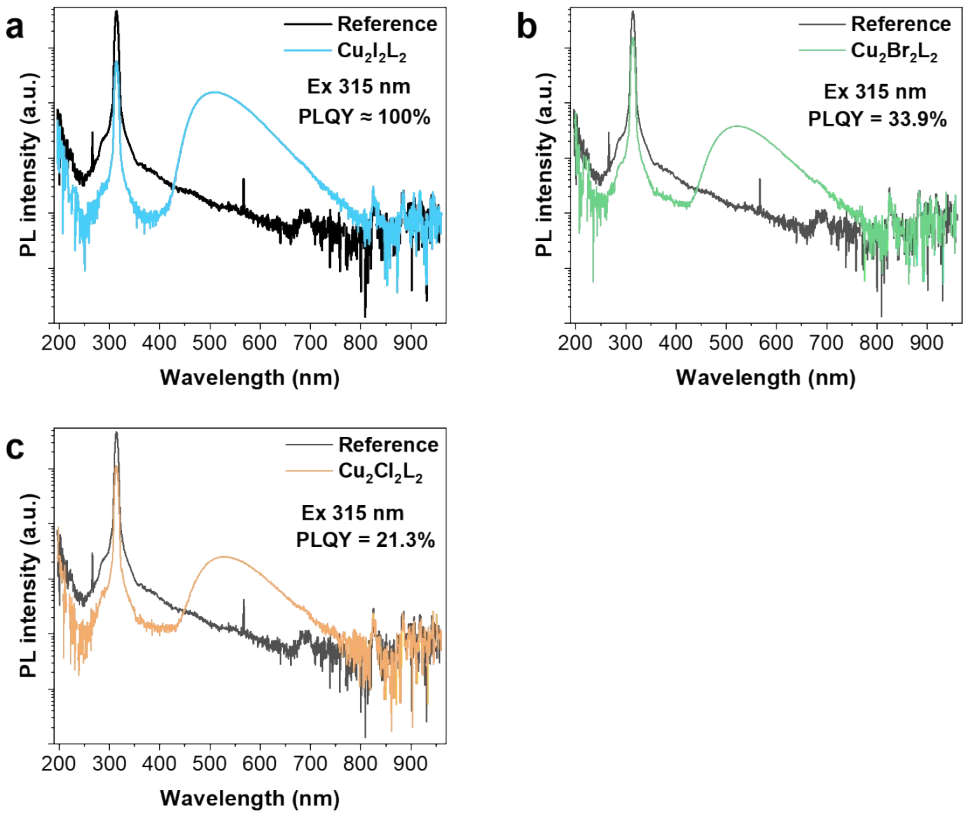

Figure S4. The PLQY curve of $Cu_2X_2L_2$ crystals under 315 nm UV excitation.

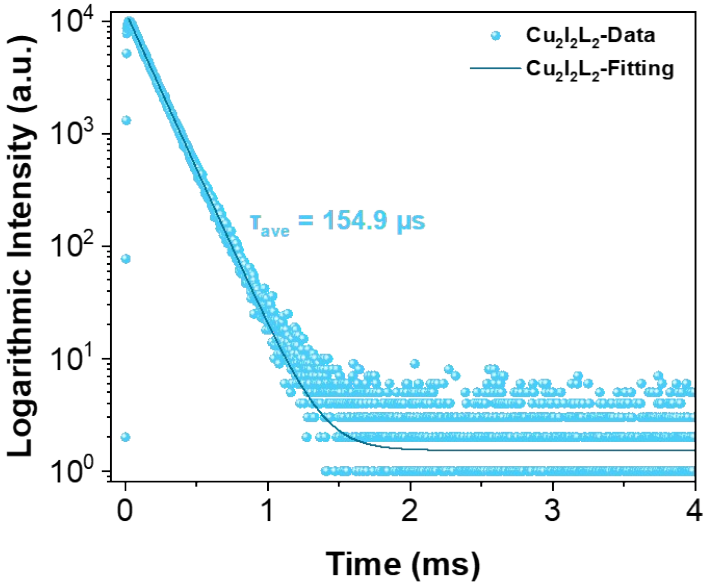

Figure S5. TRPL spectra of $Cu_2I_2L_2$.

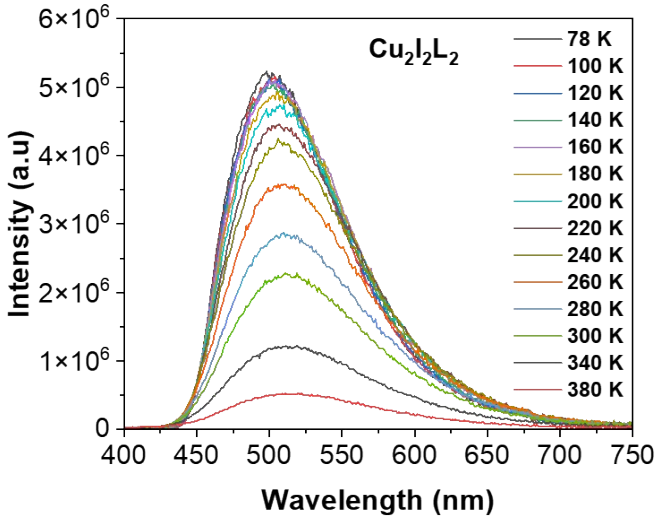

Figure S6. The PL spectra of $Cu_2I_2L_2$ over the temperature range of 78–380 K.

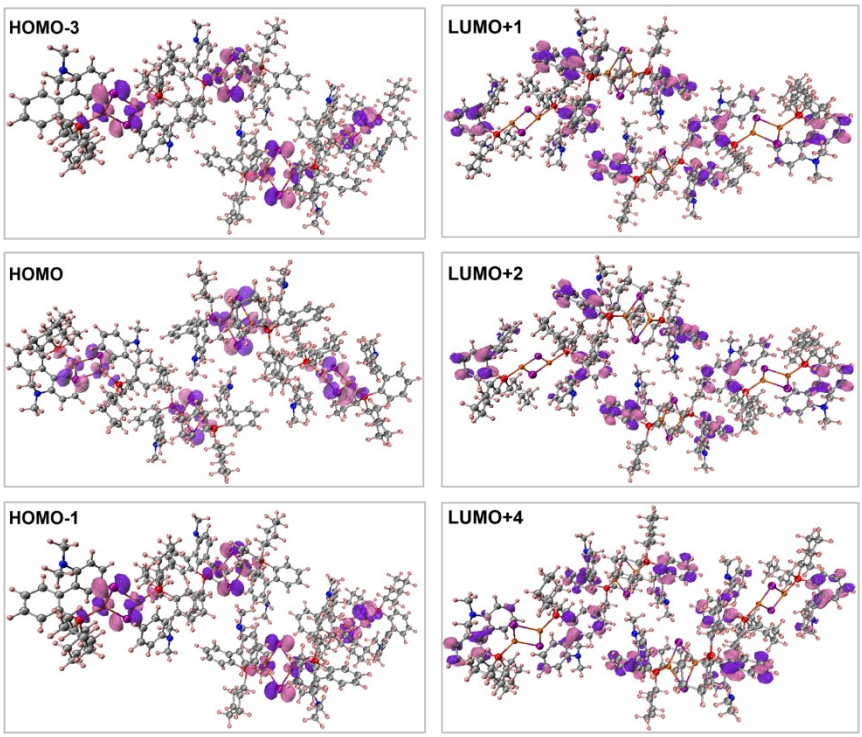

Figure S7. HOMO, HOMO-1, HOMO-3, LUMO+1, LUMO+2, and LUMO+4 distribution of $Cu_2I_2L_2$ ($S_0 \rightarrow S_1$ transition).

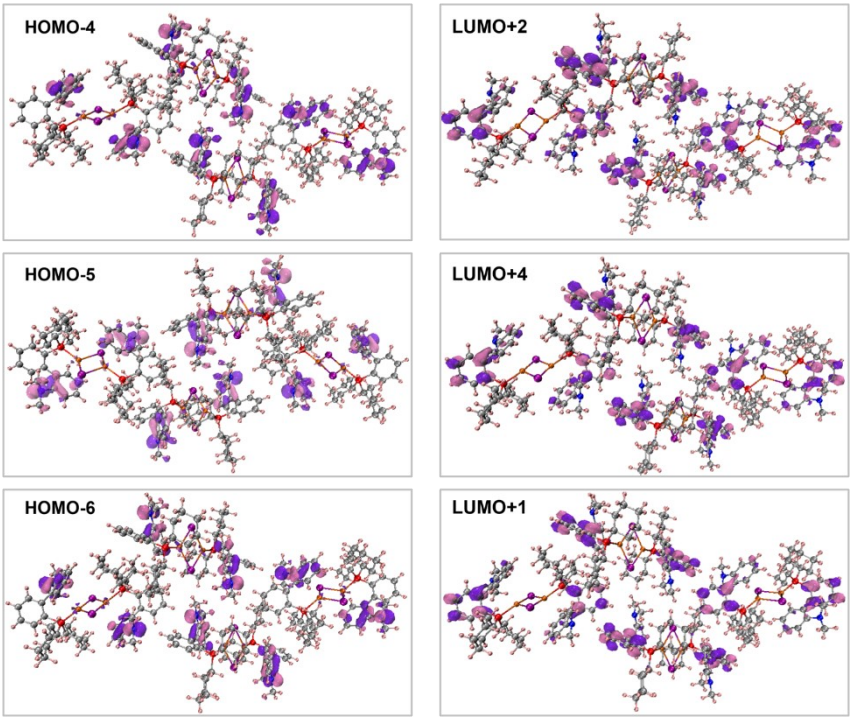

Figure S8. HOMO-4, HOMO-5, HOMO-6, LUMO+1, LUMO+2, and LUMO+4 distribution of $Cu_2I_2L_2$ ($S_0 \rightarrow T_1$ transition).

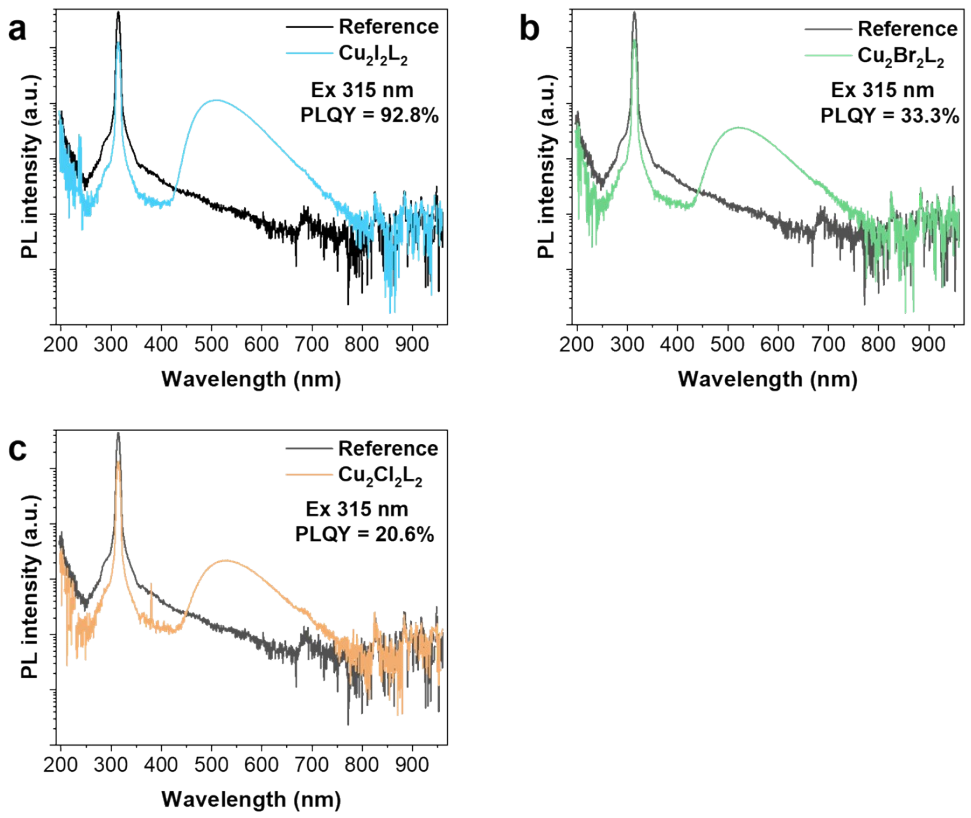

Figure S9. The PLQY curve of $Cu_2X_2L_2$ crystals under 315 nm UV excitation after being soaked in distilled water for 28 days.

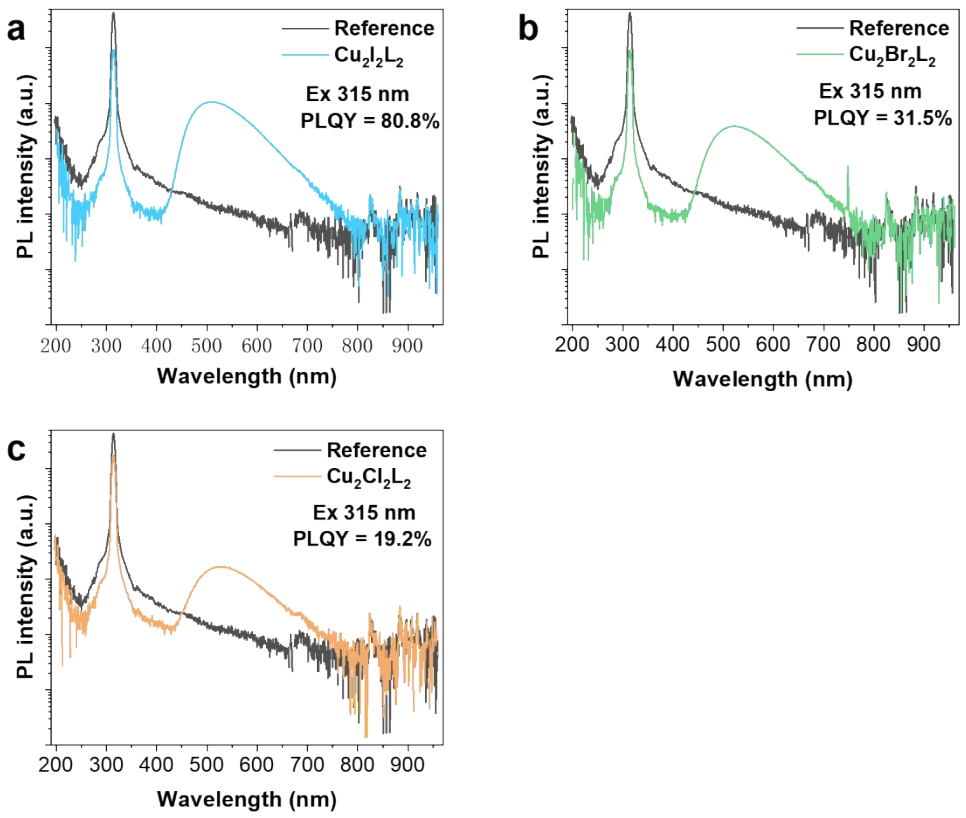

Figure S10. The PLQY curve of $Cu_2X_2L_2$-crystal under 315 nm UV excitation after being soaked in distilled water for 231 days.

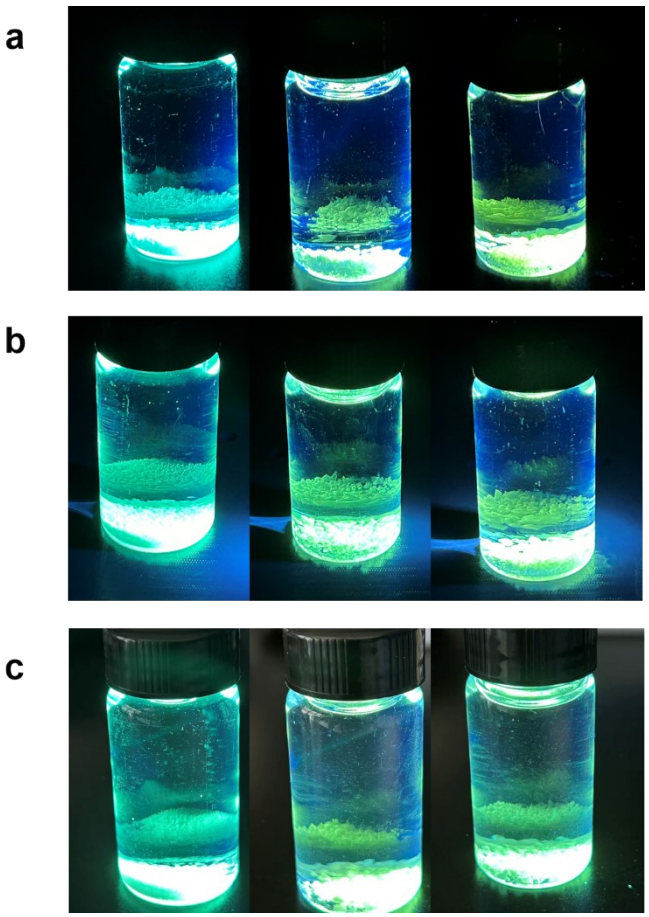

Figure S11. (a-c) Photographs of $Cu_2X_2L_2$ crystals under UV illumination (from left to right: $Cu_2I_2L_2$, $Cu_2Br_2L_2$, $Cu_2Cl_2L_2$) (a) upon initial immersion in distilled water, (b) after 28 days, and (c) after 231 days of soaking.

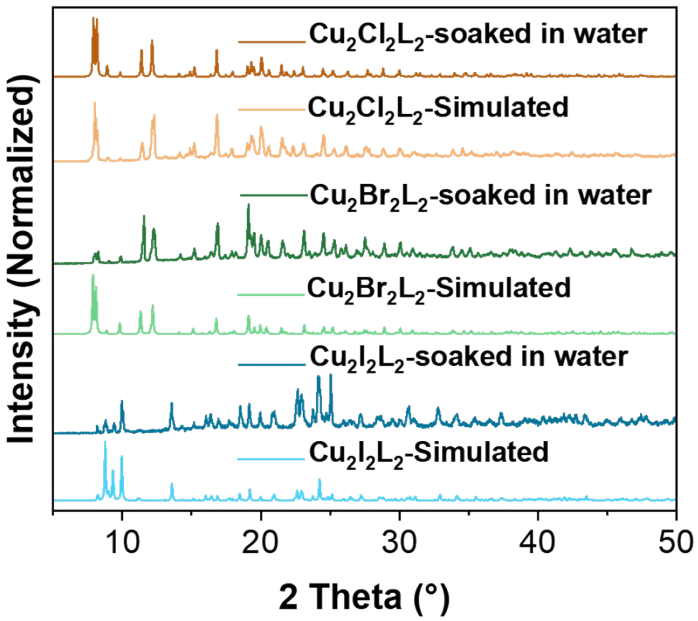

Figure S12. Simulated and PXRD patterns of $Cu_2X_2L_2$ after being soaked in distilled water for 404 days.

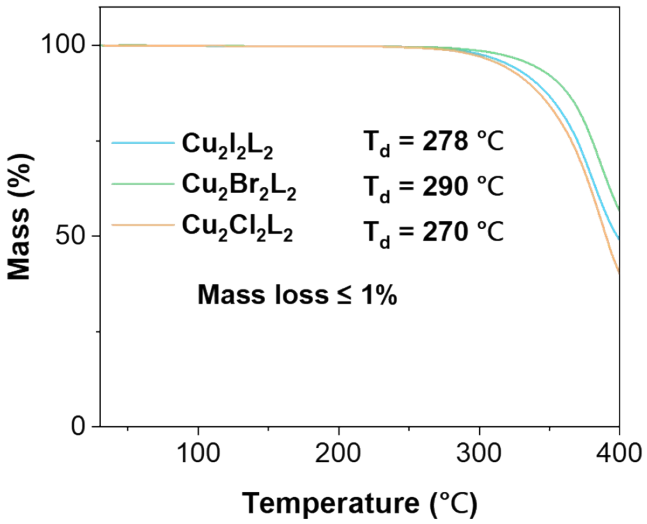

Figure S13. The TG curves of $Cu_2X_2L_2$ crystals.

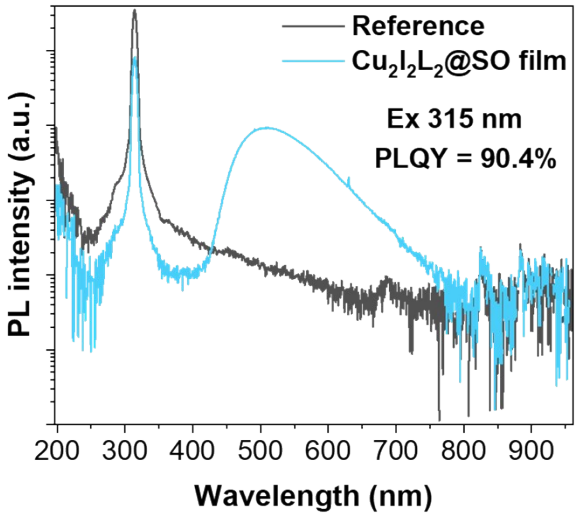

Figure S14. The PLQY curve of $Cu_2I_2L_2$ scintillator film under 315 nm UV excitation.

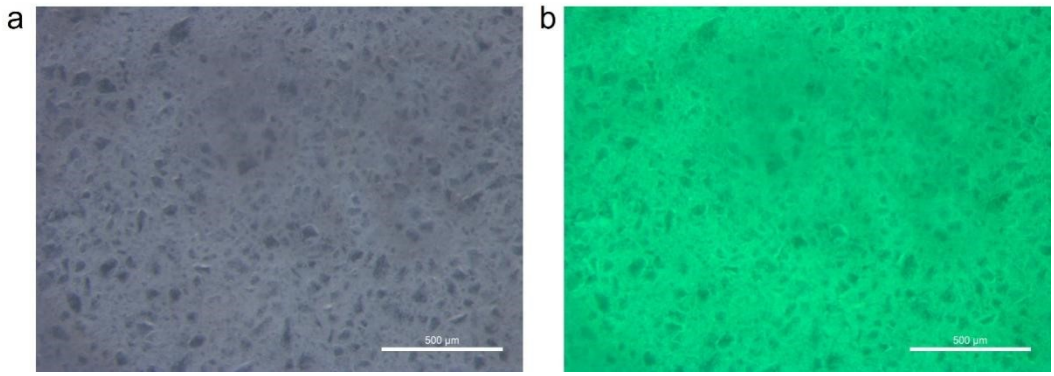

Fig. S15. The stereofluorescence microscope images of $Cu_2I_2L_2$@SO film under (a) visible and (b) UV (λ_{ex}=365 nm) light.

References

1. L.-J. Xu, X. Lin, Q. He, M. Worku and B. Ma, *Nat. Commun.*, 2020, **11**, 4329.
2. M. Wu, J. a. Lai, Y. Pu, Z. Wang, F. Kuang, Y. Zhou, K. An, S. Cao, B. Sun, Z. Liu, J. Du, H. Luo, P. He and X. Tang, *J. Mater. Chem. C*, 2025, **13**, 11764-11775.
3. S. Cao, C. Li, P. He, J. a. Lai, K. An, M. Zhou, P. Feng, M. Zhou and X. Tang, *ACS Appl. Opt. Mater.*, 2023, **1**, 623-632.
4. T. Xu, Y. Li, M. Nikl, R. Kucerkova, Z. Zhou, J. Chen, Y.-Y. Sun, G. Niu, J. Tang, Q. Wang, G. Ren and Y. Wu, *ACS Appl. Mater. Interfaces*, 2022, **14**, 14157-14164.
5. K. Han, J. Jin, B. Su, J. Qiao and Z. Xia, *Adv. Optical Mater.*, 2022, **10**, 2200865.
6. Q. Hu, C. Zhang, X. Wu, G. Liang, L. Wang, X. Niu, Z. Wang, W.-D. Si, Y. Han, R. Huang, J. Xiao and D. Sun, *Angew. Chem. Int. Ed.*, 2023, **62**, e202217784.
7. S. Cao, J. a. Lai, Y. Wang, K. An, T. Jiang, M. Wu, P. He, P. Feng and X. Tang, *J. Lumin.*, 2025, **277**.
8. J. Jiang, Y. Zhao, Z. Li, Y. Ye, Z. Wu, F. Jiang, L. Chen and M. Hong, *Angew. Chem. Int. Ed.*, 2025, **64**, e202422995.
9. W. Wu, R. Zhou, J.-X. Wang, S. Thomas, Y. Xu, X. Zhu, J. P. Jurado, X. Yuan, T. He, X. Hu, S. Wang, M. C. Faleiros, X. Li, M. Eddaoudi, H. N. Alshareef, O. M. Bakr and O. F. Mohammed, *J. Am. Chem. Soc.*, 2025, **147**, 45452-45461.